

Preparation and Properties of Fe₃O₄/SiO₂/TiO₂ Core-Shell Nanocomposite as Recoverable Photocatalyst

E.S. KUNARTI*, A. SYOUFIAN, I.S. BUDI and A.R. PRADIPTA

Department of Chemistry, Faculty of Mathematics and Natural Sciences, Universitas Gadjah Mada, Yogyakarta, Indonesia

*Corresponding author: Tel/Fax: +62 274 545188; E-mail: eko_kunarti@ugm.ac.id

Received: 28 October 2015;

Accepted: 27 January 2016;

Published online: 29 February 2016;

AJC-17805

The Fe₃O₄/SiO₂/TiO₂ nanocomposite has been prepared by coating magnetite core particles with silica and photoactive titania using sonocoprecipitation and sol-gel methods followed by microwave assisted synthesis. The nanocomposite was characterized by X-ray diffraction, infrared spectroscopic analysis, diffuse reflectance spectroscopy and transmission electron microscopy. Results showed that the product is Fe₃O₄ crystal coated with SiO₂ and TiO₂. Transmission electron microscopy image showed that core-shell structure of Fe₃O₄/SiO₂/TiO₂ has been produced. The prepared photocatalyst presented good photocatalytic activities for the degradation of methylene blue under UV irradiation. The Fe₃O₄/SiO₂/TiO₂ nanocomposite could be easily recovered by the application of external magnetic field for reuse.

Keywords: Nanocomposite, Fe₃O₄/SiO₂/TiO₂, Core-shell, Magnetic, Photocatalyst.

INTRODUCTION

Titanium dioxide, semiconductor photocatalyst, has been frequently employed in the environmental treatment and purification purposes [1-3]. Research indicates that almost any organic pollutants and many of the inorganic pollutants can be completely destroyed or separated [4-6].

Activation of TiO₂ can be achieved through the absorption of a photon from UV irradiation source. This results in the promotion of an electron (e⁻) from the valence band to the conduction band, with the generation of highly reactive positive holes (h⁺) in the valence band, causing aggressive oxidation of the surface adsorbed toxic organic pollutants [7]. However, the large-scale application of titanium dioxide as an efficient photocatalyst has been hindered by the problem of recycling the photocatalyst powders in the aqueous purification. The TiO₂ nanoparticles could be difficult to be recovered and lost readily upon being dispersed into wastewater. This problem can be overcome by modifying the TiO₂ photocatalyst by providing a magnetic property to the TiO₂ particles. Many researchers reported that the magnetic properties of TiO₂ could be obtained by coating TiO₂ on magnetic particles such as maghemite, ferrite and magnetite [8-10]. The introduction of magnetic components into TiO₂ nanoparticle-based catalysts may, therefore, enhance the separation and recovery of TiO₂ [9]. Some modifications have been made to improve the magnetic property of the TiO₂ photocatalyst. Schatz *et al.* [11] developed

a large scale synthesis of discrete and uniformly sized super paramagnetic Fe₃O₄-SiO₂. Abramson *et al.* [12] produced Fe₃O₄-SiO₂-TiO₂ nanoparticles of few tens nanometers by successively coating onto magnetic nanoparticles a SiO₂ layer and a TiO₂ layer. The magnetic modified TiO₂ was also reported could increase the photocatalytic efficiency of TiO₂. Xue *et al.* [13] found that TiO₂ coated magnetite and SiO₂ with core shell structure could successfully degrade 80 % of methyl orange under visible irradiation for 90 min. The magnetic composite photocatalyst can be easily recovered from the aqueous solution by applying an external magnetic field.

Many methods have been applied to prepare composites with core-shell structure such as sol-gel methods and the most frequently used are hydrothermal synthesis [14-17]. Although the composites have been prepared successfully *via* these methods, however, there are currently few literature reported on the synthesis of Fe₃O₄/SiO₂/TiO₂ core-shell nanoparticles and their photocatalytic properties. The reported synthesis methods were generally complicated and time consuming [18]. Therefore it remains a great challenge to explore a practicable method for the preparation of core-shell nanostructure composites to maximize the photocatalytic efficiency. Present trend in synthetic techniques moves from just achieving of product with desired properties to green methods that are effective, economic and environmental friendly. In the present study, we report the simple preparation of TiO₂ coated Fe₃O₄-SiO₂ nanocomposite as a magnetically recoverable

photocatalyst using sol-gel process and microwave-assisted synthesis.

EXPERIMENTAL

Iron(II) chloride tetrahydrate (Merck); iron(III) chloride hexa-hydrate (Merck); tetraethyl orthosilicate (TEOS, 99.3 %, Merck); oleic acid (Chemix Lab); absolute ethanol (97.0 %, Merck); ammonia solution (25 %, Merck); titanium(IV) tetraisopropoxide (TTIP, 97 %, Aldrich); and deionized water, were used throughout the experiment. All chemicals were used as received without further purification.

Synthesis of magnetite (Fe₃O₄) nanoparticles: Iron(III) chloride hexa-hydrate (FeCl₃·6H₂O, 5.41 g) and FeCl₂·4H₂O (2.78 g) were dissolved in 100 mL of deionized water under the control of nitrogen gas. The solution was ultrasonicated and added drop-wise of aqueous solution of NH₄OH 25 % (30 mL). Oleic acid (1 g) were then added to the solution and ultrasonicated for 1 h. The precipitate was then collected, washed with deionized water and dried at 80 °C for overnight

Synthesis of Fe₃O₄/SiO₂: The magnetite particles (0.5 g) were suspended in 60 mL ethanol and sonicated for 20 min. TEOS, preliminarily diluted in ethanol, was added drop-wise to the magnetite particle suspension. Then an aqueous solution of NH₄OH (25 %) was added and the TEOS hydrolysis and condensation was allowed under overnight gentle stirring. The obtained magnetite particles covered by a silica layer were washed with deionized water until neutral. The residue was separated with external magnetic field then dried at 80 °C and heated under microwave irradiation for 3 min at a power of 600 watt.

Synthesis of Fe₃O₄/SiO₂/TiO₂: Fe₃O₄/SiO₂ nanoparticles (200 mg) were dispersed in ethanol 97 % (30 mL), followed by the addition of TTIP (1 mL) and deionized water (0.1 mL). The mixture was then stirred for 8 h. The obtained nanoparticles were washed with deionized water. The residue was separated using external magnetic field, dried and calcined under microwave irradiation for 15 min using a power of 600 watt.

Characterization: Fourier transform infrared (FT-IR) spectra were recorded on a Shimadzu FTIR-8201 PC spectrophotometer using KBr pellets for samples. X-ray diffraction (XRD) patterns were analyzed by X-ray diffractometer (Shimadzu 6000) using Cu K_α radiation source at 35 kV, with a scan rate of 0.1° 2θ s⁻¹ in the 2θ range of 10-80°. The morphology and microstructure of products were characterized by transmission electron microscopy (TEM) measurements (JEOL JEM-1400EX) with the working voltage of 120 kV. Diffuse reflectance spectra were recorded by UV-visible spectrophotometer (Shimadzu 2450, with double beam system, equipped with diffuse reflectance spectroscopic accessories).

Photocatalytic activity test: The photocatalytic activity of Fe₃O₄/SiO₂/TiO₂ nanocomposite was examined by the photodegradation of an aqueous solution of methylene blue under UV irradiation. The photodegradation experiments were carried out in a closed box equipped with ultraviolet light (40 W, Philips). About 25 mg/L methylene blue solution (10 mL) and 0.05 g of Fe₃O₄/SiO₂/TiO₂ nanocomposite were placed inside a glass vial. During the photocatalytic reaction, the nanocomposites were dispersed by stirring the suspension

continuously. After photodegradation, the absorbance of the solution was analyzed by UV-visible spectrophotometer at the optimum absorption wavelength of methylene blue (642 nm).

RESULTS AND DISCUSSION

The structure of the Fe₃O₄, Fe₃O₄/SiO₂ and Fe₃O₄/SiO₂/TiO₂ nanocomposites were characterized by using FT-IR spectroscopy and X-Ray diffraction methods with the infrared spectra were shown in Fig. 1. There are some signals indicated absorption bands of Fe₃O₄. These include vibration band at the wave number of 570 cm⁻¹ corresponds to the stretching vibration of Fe-O, 1527 cm⁻¹ indicate the presence of asymmetric vibration group of COO⁻ and 2337 cm⁻¹ for N-H stretching mode. The magnetite Fe-O bond absorption intensity tends to decrease after coating process as the magnetite surfaces were covered by either SiO₂ itself or SiO₂ and TiO₂. This indicates the perfect coating is formed. Some additional signals appear on Fe₃O₄/SiO₂ and Fe₃O₄/SiO₂/TiO₂ spectra, such as a symmetric stretching vibration of Si-O from Si-O-Si at the wave number of 800 cm⁻¹, asymmetric stretching vibration of Si-O from Si-O-Si at 1090 cm⁻¹, Si-O stretching vibration due to Si-O-Ti at 960-940 cm⁻¹ and the vibration band for the fingerprint of Ti-O-Ti bond at around 700-500 cm⁻¹. The presence of water is evidenced by the appearance of the bending mode at 1620 cm⁻¹ and the stretching mode at 3372 cm⁻¹.

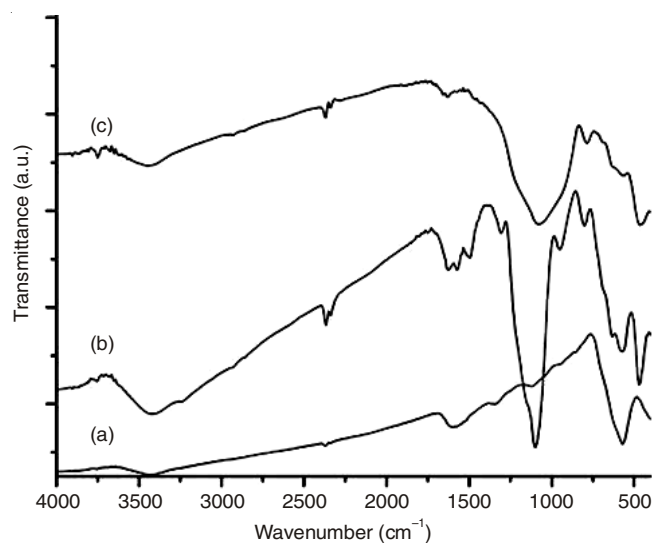


Fig. 1. Infrared spectra of (a) Fe₃O₄, (b) Fe₃O₄/SiO₂ and (c) Fe₃O₄/SiO₂/TiO₂

Fig. 2 depicts the X-ray diffraction pattern of the samples. Some characteristic peaks at 30.18; 35.70; 43.37; 57.22 and 62.86° were detected (Fig. 2a), indicating that the Fe₃O₄ was successfully prepared. No significantly different in diffraction data was observed between the SiO₂ coated magnetite (Fig. 2b) and the Fe₃O₄ samples. The broad peak at around 20° may indicate the presence of the amorphous SiO₂. The diffraction pattern of Fe₃O₄/SiO₂/TiO₂ (Fig. 2c) shows a new peak of anatase TiO₂ at 25, 27° confirms the successful of TiO₂ coating. The reduction of Fe₃O₄ peaks also indicates the perfect TiO₂ coating. This result is in agreement with Fe₃O₄/SiO₂ and Fe₃O₄/SiO₂/TiO₂ samples reported by other studies [11-13].

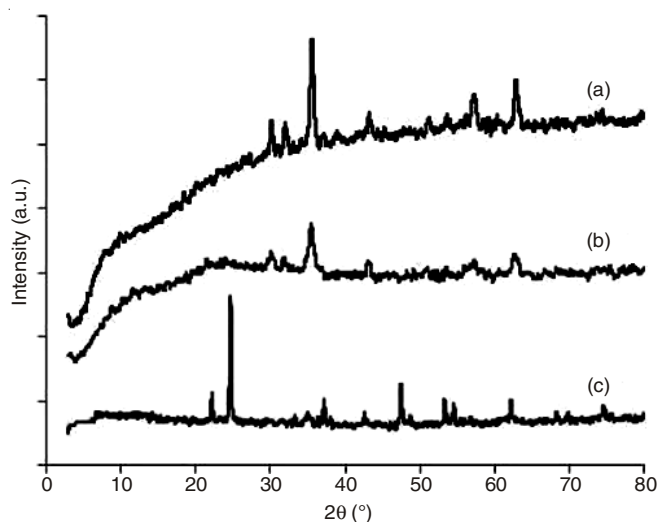


Fig. 2. X-ray diffraction pattern of (a) Fe₃O₄, (b) Fe₃O₄/SiO₂ and (c) Fe₃O₄/SiO₂/TiO₂

Fig. 3(a) is the TEM image of Fe₃O₄/SiO₂ particles. It can be seen that there is a thin bright layer around the dark contrast Fe₃O₄ nanoparticles which can be observed clearly and this is probably the SiO₂ layer. The image also shows that the Fe₃O₄/SiO₂ composites consist of spherical particles with sizes around 12–15 nm. Moreover, a large number of Fe₃O₄ nanoparticles were encapsulated within the SiO₂ shell with the mean diameters of Fe₃O₄/SiO₂ core-shell approximately 30 nm. The TEM image of Fe₃O₄/SiO₂/TiO₂ nanocomposite is shown as Fig. 3(b). It clearly displays that TiO₂ was successfully coated on Fe₃O₄/SiO₂ particles. The results show that core-shell Fe₃O₄/SiO₂/TiO₂ functional nanocomposites have been successfully synthesized. Similar observations have been reported by Pang *et al.* [18] for sample prepared by sol-gel method followed by calcination for 3 h. They found that the core-shell structure of Fe₃O₄/SiO₂/TiO₂ with the particle size were around 90 nm. In this work, smaller particles (30 nm) were obtained by using sol-gel method and microwave assisted synthesis.

Fig. 4 shows the ultraviolet-visible absorption spectra of the Fe₃O₄/SiO₂/TiO₂ particles and pure TiO₂ particles. The absorption spectrum of TiO₂ has a strong peak between 200 and 400 nm, corresponding to the band edge absorption of light by titania. Similar absorption spectrum was observed for the Fe₃O₄/SiO₂/TiO₂ nanocomposite sample. It seems that the introduction of the Fe₃O₄ core did not significantly alter the core-shell particles' absorption spectrum pattern. The absorption edge of TiO₂ in the nanocomposite was 378 nm, with the band gap energy around 3.29 eV. This result suggests that the Fe₃O₄/SiO₂/TiO₂ nanocomposites obtained in this study might be suitable to have high efficiency for photocatalytic in ultraviolet region.

In order to demonstrate the photocatalytic activity of the Fe₃O₄/SiO₂/TiO₂ nanocomposites, methylene blue in aqueous solution was photooxidized under UV light irradiation. Fig. 5 displays the photocatalytic activity of the nanocomposites at pH 8 with various irradiation time. It shows that the nanocomposites gave a good performance as photocatalyst with the degradation yield was higher than that of pure TiO₂. This may be attributed to rough and porous surface of Fe₃O₄/SiO₂/TiO₂ composites, which enhances the photocatalytic activity by

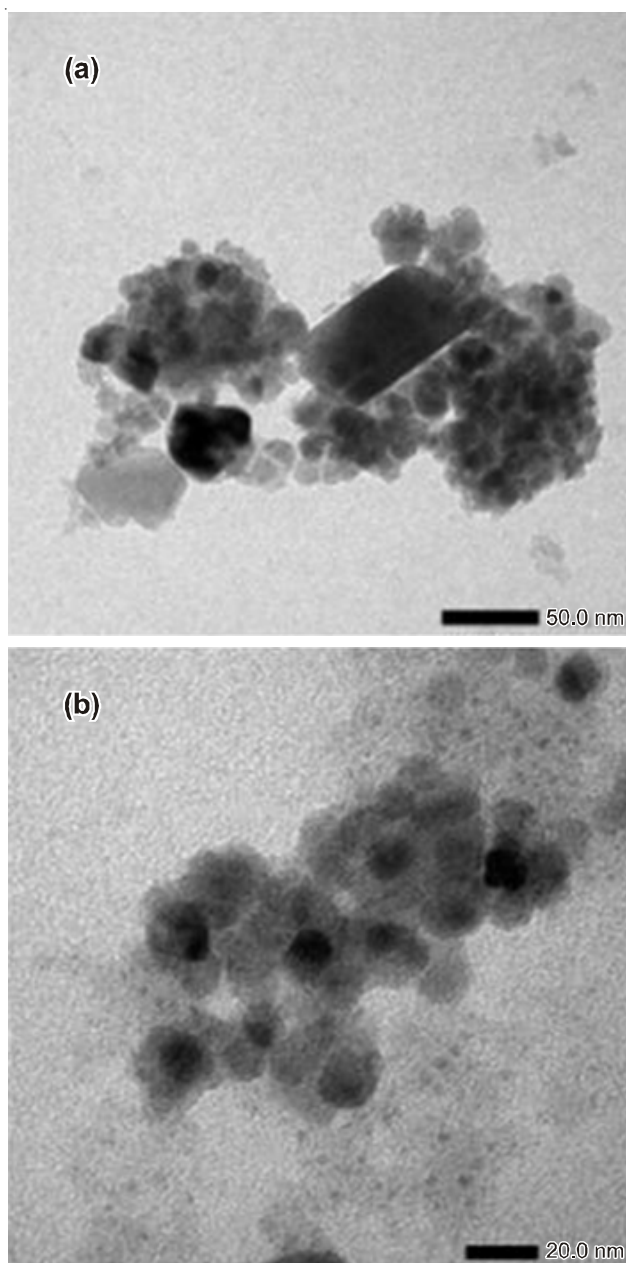


Fig. 3. TEM images of (a) Fe₃O₄/SiO₂ and (b) Fe₃O₄/SiO₂/TiO₂

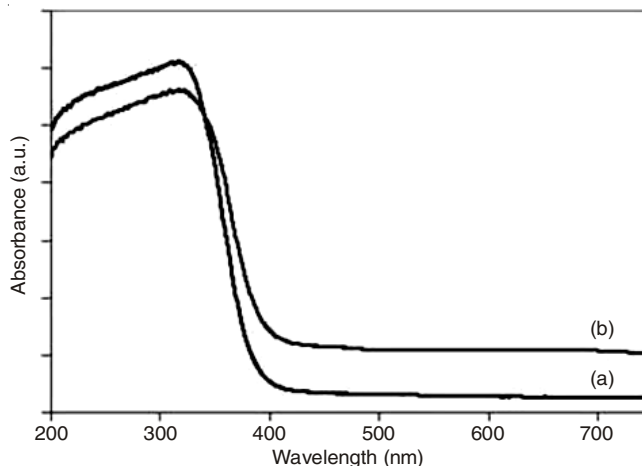


Fig. 4. UV-visible diffuse reflectance spectra of (a) TiO₂ and (b) Fe₃O₄/SiO₂/TiO₂

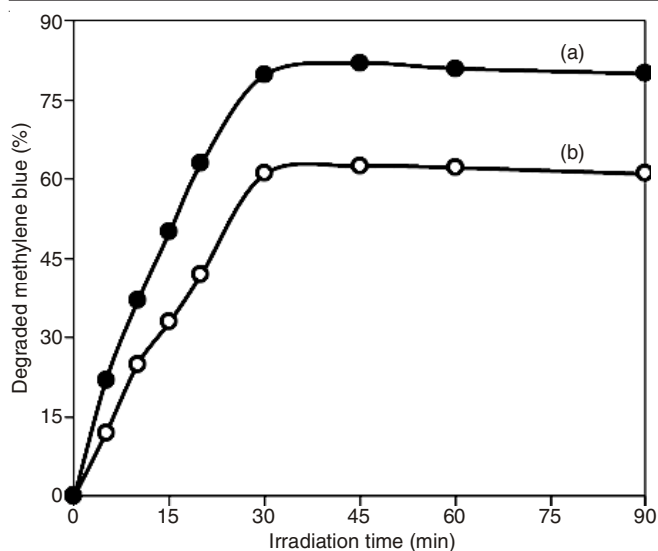


Fig. 5. Photodegradation of methylene blue at a pH of 8, photocatalyzed by (a) Fe₃O₄/SiO₂/TiO₂ and (b) TiO₂

facilitating the access to the reactive TiO₂. It may also be ascribed to the decreasing size of TiO₂ in the Fe₃O₄/SiO₂/TiO₂ nanocomposites resulted in the increased effective TiO₂ surface area. Another reason is probably due to the nanosized TiO₂ particles possess a larger band-gap with a higher photooxidation capability, hence the strong oxidizing potential of the photo-generated holes has made by the nanocomposites for oxidation reactions.

Conclusion

Titanium dioxide was successfully coated onto seed magnetic particles Fe₃O₄/SiO₂ via a simple sol gel processing followed by microwave assisted synthesis. The Fe₃O₄ nanoparticles were encapsulated within silica spheres and a layer of TiO₂ shell was then coated onto silica. The Fe₃O₄/SiO₂/TiO₂ nanocomposites show excellent magnetism and higher photocatalytic activity than pure TiO₂ attributed to rough and porous

surface of Fe₃O₄/SiO₂/TiO₂ nanocomposites. The nanocomposites could degrade 82.40 % within 30 min of methylene blue 25 mg/L. The nanocomposite can be retrieved from the reaction mixture by simple magnetic separation.

ACKNOWLEDGEMENTS

The authors acknowledge to The Directorate General of Higher Education, Ministry of Research Technology and Higher Education Republic of Indonesia and Universitas Gadjah Mada for the financial support.

REFERENCES

1. M.R. Hoffmann, S.T. Martin, W. Choi and D.W. Bahnemann, *Chem. Rev.*, **95**, 69 (1995).
2. S. Yin, B. Liu, P.L. Zhang, T. Morikawa, K. Yamanaka and T. Sato, *J. Phys. Chem. C*, **112**, 12425 (2008).
3. H. Taoda, *Res. Chem. Intermed.*, **34**, 417 (2008).
4. M.H. Habibi, S. Tangestaninejad and B. Yadollahi, *Appl. Catal. B*, **33**, 57 (2001).
5. X. Chen and S.S. Mao, *Chem. Rev.*, **107**, 2891 (2007).
6. V. Mirkhani, S. Tangestaninejad, M. Moghadam, M.H. Habibi and A. Rostami-Vartooni, *J. Iran. Chem. Soc.*, **6**, 578 (2009).
7. W. Choi, *Catal. Surv. Asia*, **10**, 16 (2006).
8. Y. Gao, B. Chen, H. Li and Y. Ma, *Mater. Chem. Phys.*, **80**, 348 (2003).
9. M. Ye, Q. Zhang, Y. Hu, J. Ge, Z. Lu, L. He, Z. Chen and Y. Yin, *Chem. Eur. J.*, **16**, 6243 (2010).
10. Y. Ruzmanova, M. Stoller and A. Chianese, *Chem. Eng. Trans.*, **32**, 2269 (2013).
11. A. Schatz, M. Hager and O. Reiser, *Adv. Funct. Mater.*, **19**, 2109 (2009).
12. S. Abramson, L. Srithammavanh, J.-M. Siaugue, O. Horner, X. Xu and V. Cabuil, *J. Nanopart. Res.*, **11**, 459 (2009).
13. C. Xue, Q. Zhang, J. Li, X. Chou, W. Zhang, H. Ye, Z. Cui and P.J. Dobson, *J. Nanomater.*, **Article ID 762423** (2013).
14. Y.X. Zhang, G.H. Li, Y.X. Jin, Y. Zhang, J. Zhang and L.D. Zhang, *Chem. Phys. Lett.*, **365**, 300 (2002).
15. L.M. Sikhivhilu, S. Sinha Ray and N.J. Coville, *Appl. Phys., A Mater. Sci. Process.*, **94**, 963 (2009).
16. B. Roy and P.A. Fuierer, *J. Am. Ceram. Soc.*, **93**, 436 (2010).
17. D.L. Morgan, G. Triani, M.G. Blackford, N.A. Raftery, R.L. Frost and E.R. Waclawik, *J. Mater. Sci.*, **46**, 548 (2011).
18. S.C. Pang, S.Y. Kho and S.F. Chin, *J. Nanomater.*, **Article ID 427310** (2012).